Angewandte Chemie
Eine Zeitschrift der Gesellschaft Deutscher Chemiker

Supporting Information

69451 Weinheim, Germany

Mechanism of Multivalent Carbohydrate–Protein Interactions Studied by EPR Spectroscopy**

Patrick Braun, Bettina Nägele, Valentin Wittmann, and Malte Drescher*

anie_201101074_sm_miscellaneous_information.pdf

Supporting Information

Contents

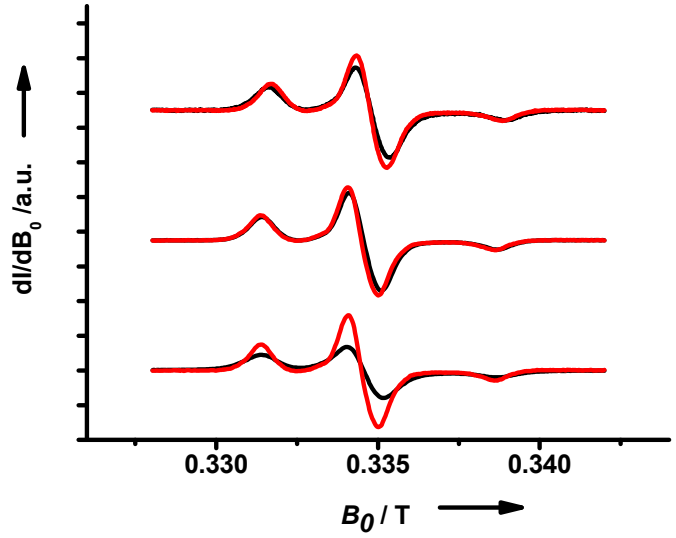

Figure S1. Comparison of cw EPR spectra at T = 120 K of singly ($\mathbf{1_1}$, red) and doubly labeled ($\mathbf{1_2}$, black) ligand **1** in absence (bottom) and in presence of WGA (molar ratio WGA dimer/ligand 8:1 (center) and 1:4 (top)). In absence of WGA, the line broadening due to dipolar coupling for $\mathbf{1_2}$ verifies significant contributions in the distance distribution below 1.5 nm while in presence of an excess of WGA those distances cannot be detected.

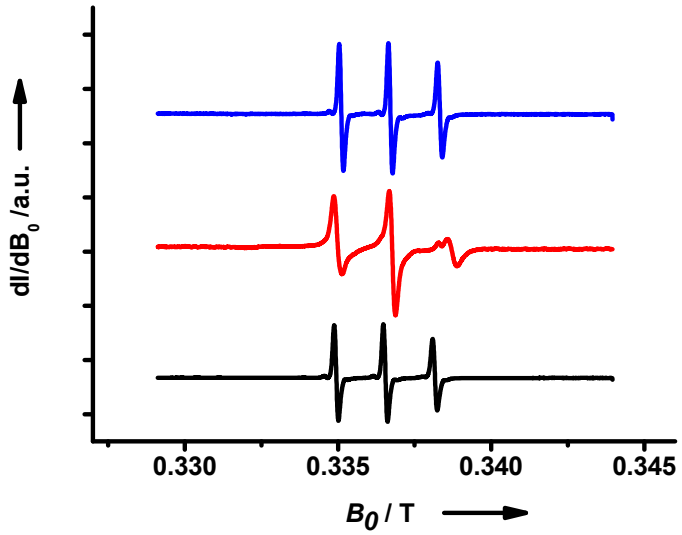

Figure S2. cw EPR spectra of $\mathbf{1_1}$ at T = 295 K. Bottom: Spectrum in absence of WGA; a rotational correlation time τ_C of 120 ps was derived by spectral simulations. Center: In presence of an excess of WGA (molar ratio WGA dimer/ligand $\mathbf{1_1}$ 8:1), the mobility of $\mathbf{1_1}$ is significantly reduced to τ_C = 1.8 ns indicating near quantitative binding. Top: For a molar WGA dimer/ligand $\mathbf{1_1}$ ratio of 1:4, the bound component with a broad line width cannot be identified in the presence of the mobile and intense spectral contribution of the unbound fraction. However, compared to the spectrum in absence of the protein (bottom, τ_C = 120 ps), an effective correlation time of τ_C = 160 ps suggests partial binding.

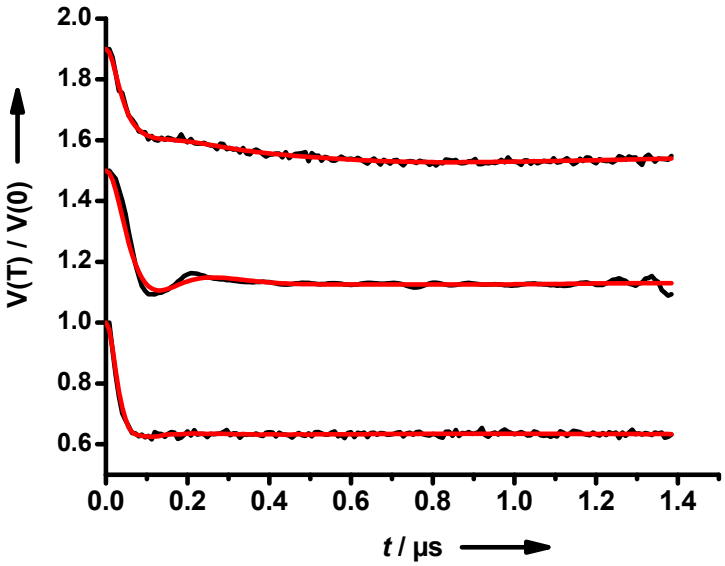

Figure S3. Baseline-subtracted DEER data for $\mathbf{1_2}$ (black) derived from experimental DEER curves after background correction and simulated curves (red) corresponding to distance distributions shown in Figure 2 obtained by Tikhonov regularization. Bottom: in absence of WGA; center: in presence of WGA (molar ratio WGA dimer/ligand $\mathbf{1_2}$ 8:1, offset 0.5); top: in presence of WGA (molar ratio WGA dimer/ligand $\mathbf{1_2}$ 1:4, offset 0.9).

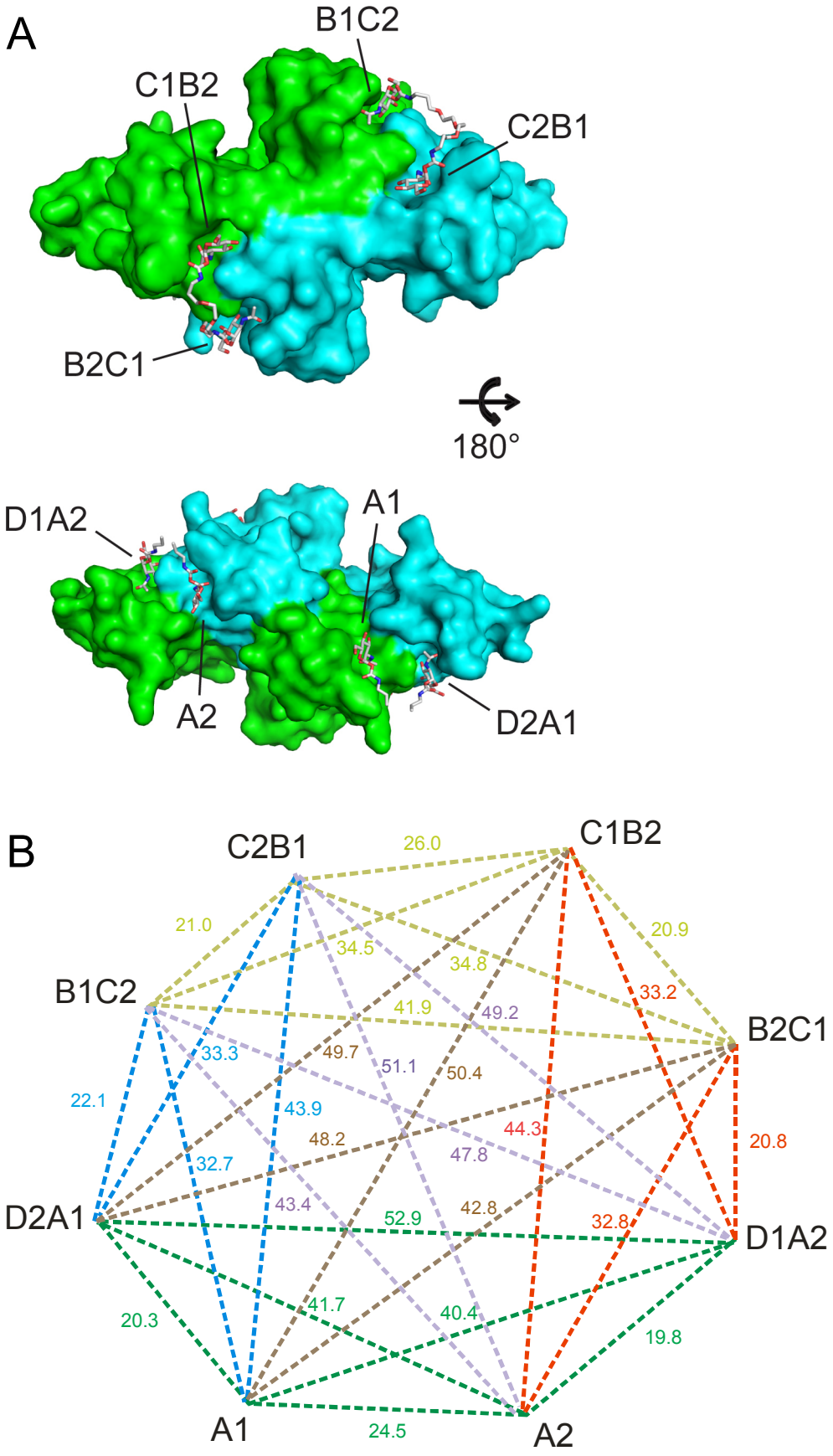

Figure S4. (A) Crystal structure of the complex of **1** and WGA (PDB ID: 2X52[1]) (B) Distances (in Å) between oxygens in the 6-position of the GlcNAc residues bound to the WGA binding sites as derived from the crystal structure 2X52.

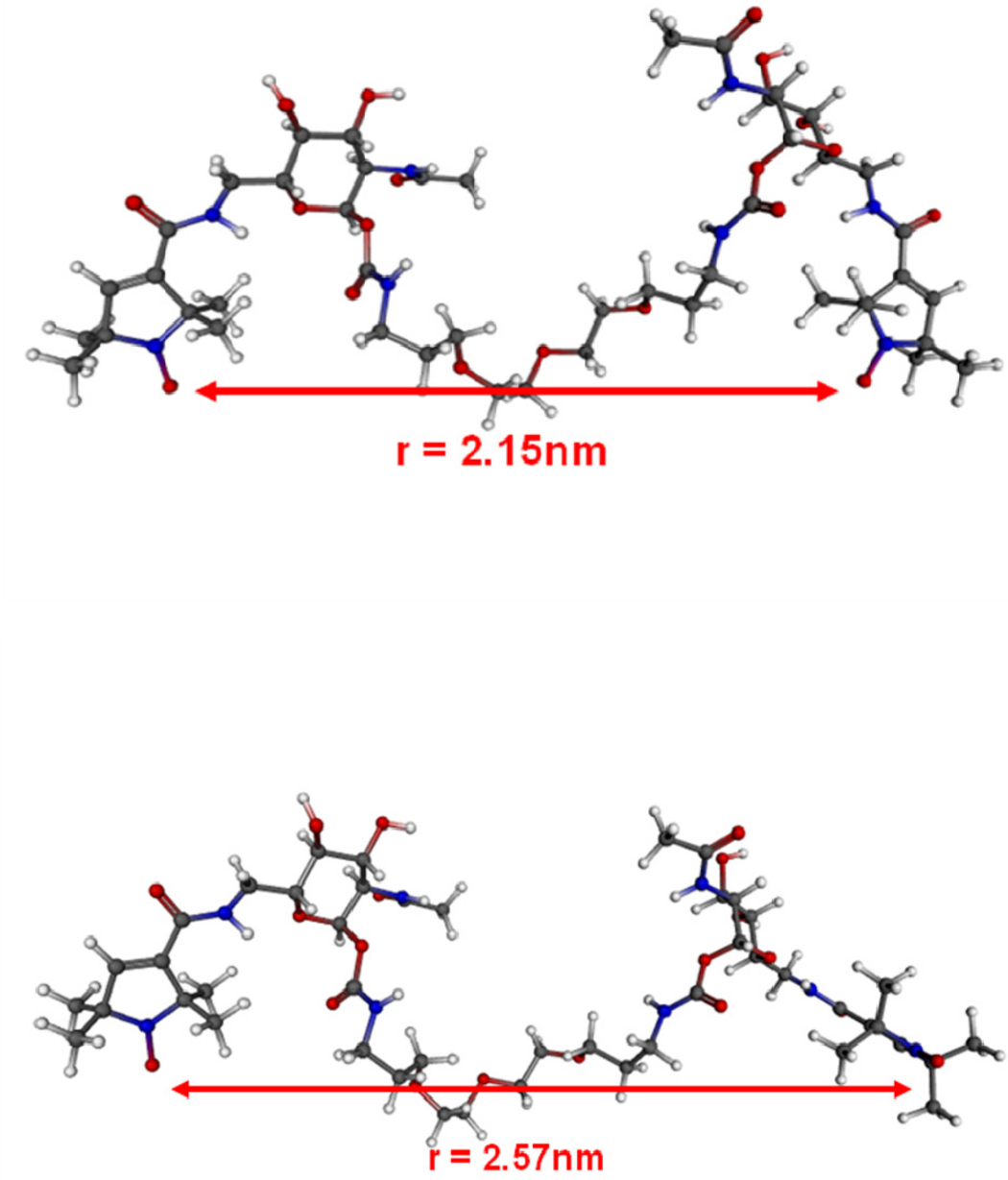

Figure S5. Top: Molecular modeling of $\mathbf{1}_2$: The conformation of **1** bound to WGA was taken from the crystal structure (Figure S4 A), the hydroxy groups in the 6-positions of the GlcNAc residues were replaced by the energy minimized spin labels. In order to estimate the width of the spin-spin distance distribution, the distance between the oxygen of the nitroxy groups was monitored versus rotation around the C_5–C_6 bonds. Two extreme cases are depicted.

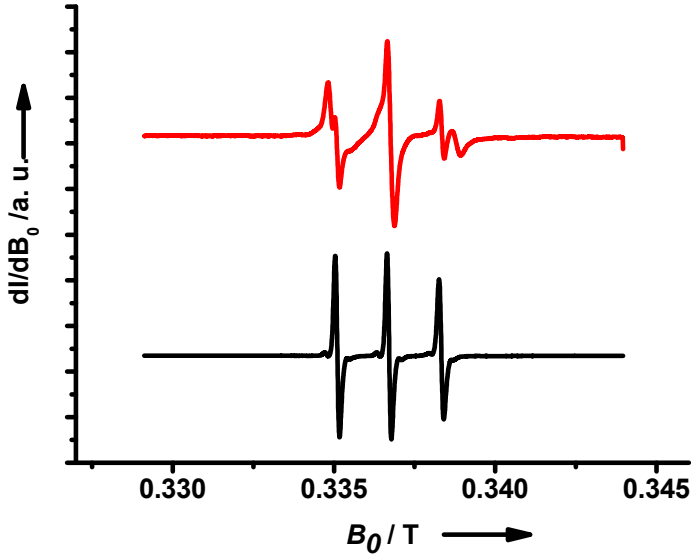

Figure S6. cw EPR spectra at T = 295 K of $\mathbf{2_1}$ in absence (bottom) and presence of WGA (molar ratio WGA dimer/ligand $\mathbf{2_1}$ 8:1, top). In absence of protein, a rotational correlation time of τ_C = 120 ps was determined. Upon addition of WGA, the main component of the spectrum corresponds to maintained mobility and only a fraction to significantly reduced mobility indicating only partial binding.

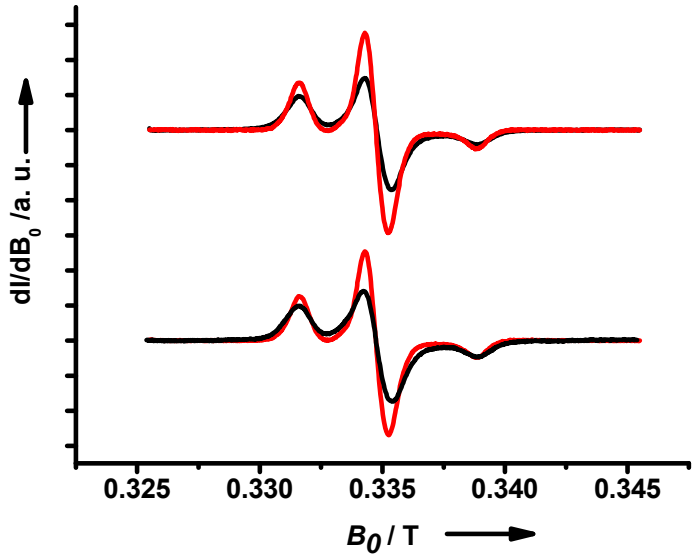

Figure S7. Comparison of cw EPR spectra at T = 120 K of singly ($\mathbf{2_1}$, red) and doubly labeled ($\mathbf{2_2}$, black) ligand **2** in absence (bottom) and in presence of WGA (molar ratio WGA dimer/ligand 8:1, top). In both spectra, the line broadening due to dipolar coupling observed for $\mathbf{2_2}$ verifies significant contributions in the distance distribution below 1.5 nm.

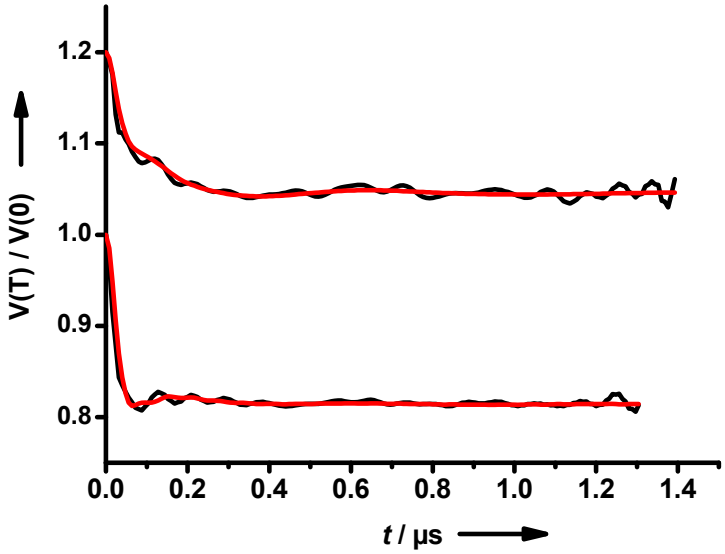

Figure S8. Baseline-subtracted DEER data for $\mathbf{2_2}$ (black) derived from experimental DEER curves after background correction and simulated curves (red) corresponding to distance distributions shown in Figure 4 obtained by Tikhonov regularization. Bottom: in absence of WGA; top: in presence of WGA (molar ratio WGA dimer/ligand $\mathbf{2_2}$ 8:1, offset 0.2).

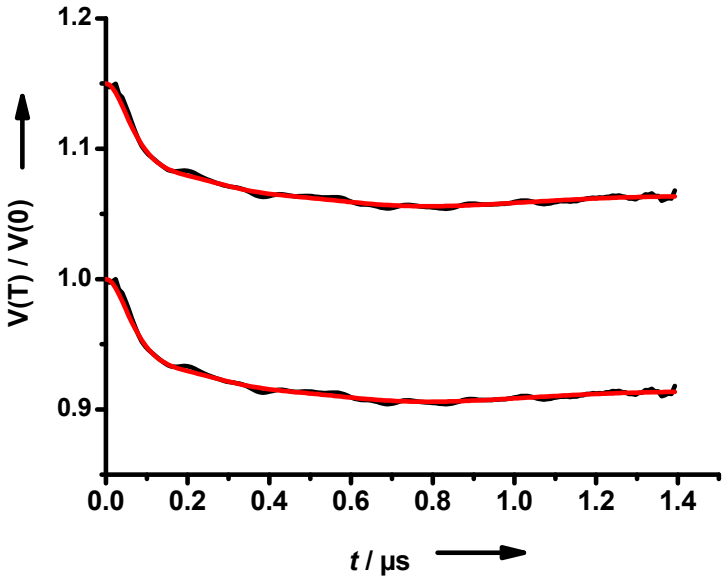

Figure S9. Baseline-subtracted DEER data for **3** in presence of WGA (black, molar ratio WGA dimer/ligand **3** 1:1 (bottom) and 1:7 (top, offset 0.2)) derived from experimental DEER curves after background correction and simulated curves (red) corresponding to distance distributions shown in Figure 5 obtained by Tikhonov regularization. While for all DEER experiments τ_1 values were incremented, the lower curve suffers from strong proton modulation due to low modulation depth. This resulted in an artifact at r = 1.5 nm for which the distance distribution shown in Figure 5 was corrected in the data post processing.

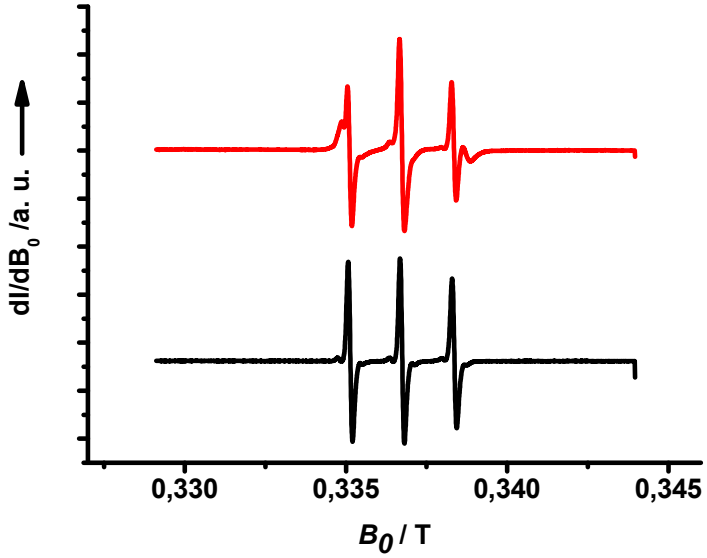

Figure S10. cw EPR spectra at T = 295 K of monovalent ligand $\mathbf{3_1}$ in absence (bottom) and presence of WGA (molar ratio WGA dimer/ligand $\mathbf{3_1}$ 8:1, top). In absence of protein, a rotational correlation time of τ_C = 120 ps was determined. Upon addition of WGA, the main component of the spectrum corresponds to maintained mobility and only a fraction to significantly reduced mobility indicating only partial binding.

Synthesis of spin-labeled WGA ligands

*Synthesis of azide-substituted glycosyl carbonate **8***

Scheme S1 depicts the synthesis of azide-substituted glycosyl carbonate **8**. Starting from *N*-acetylglucosamine **4**, selective tosylation of the primary hydroxy group followed by acetylation gave tosylate **5**. The azide was introduced by reaction with sodium azide, and **6** was selectively deprotected at the anomeric centre and subsequently reacted with *p*-nitrophenyl chloroformate to give **8**.

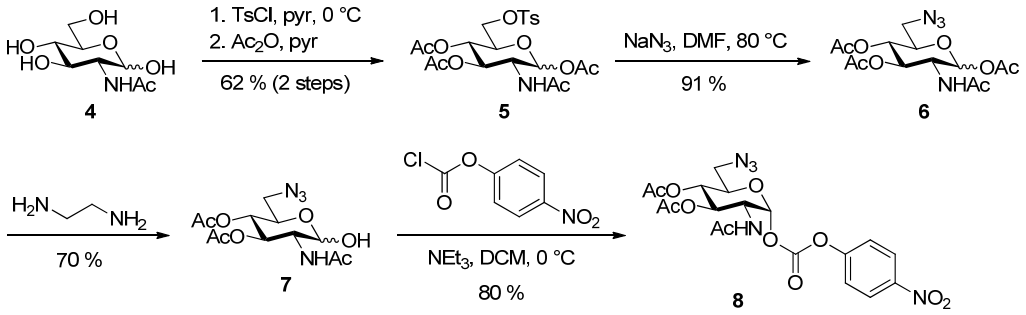

Scheme S1. Synthesis of glycosyl carbonate **8**.

*Selected analytical data of **8***

^{1}H NMR (400 MHz, $CDCl_3$): δ = 8.25 (d, J = 8.8 Hz, 2 H, H^{arene}), 7.39 (d, J = 9.7 Hz, 2 H, H^{arene}), 6.14 (d, J = 3.6 Hz, 1 H, H-1), 5.5 (d, J = 8.7 Hz, 1 H, NH), 5.25 (t, J = 10.1 Hz, 20.8 Hz, 1 H, H-3), 5.14 (t, J = 9.7 Hz, 1 H, H-4), 4.49-4.43 (m, 1 H, H-2), 4.08-4.03 (m, 1 H, H-5), 3.34-3.31 (m, 2 H, H-6), 2.01 (s, 6 H, 2 x CH_3), 1.92 (s, 3 H, CH_3); ^{13}C NMR (400 MHz, $CDCl_3$): δ = 171.7, 170.2, 169.2 (3 x $\underline{C}(O)CH_3$), 154.9 (OC(O)O), 150.6, 145.7, 125.5,121.5 (4 x C^{arene}), 95.5 (C-1), 71.5 (C-5), 70.0 (C-3), 68.3 (C-4), 51.4 (C-2), 50.6 (C-6), 23.1, 20.7, 20.6 (3 x C(O)$\underline{C}H_3$); ESI-MS: calcd for $C_{19}H_{21}N_5NaO_{11}$ m/z 518.1 $[M + Na]^+$, found 518.2.

Synthesis of singly spin-labeled ligands $\mathbf{1}_1$ and $\mathbf{2}_1$

For the synthesis of the singly labeled ligands $\mathbf{1}_1$ and $\mathbf{2}_1$, glycosyl carbonate **9**[1] was coupled to the mono Boc protected diamines **10** and **11**, respectively (Scheme S2). The formed carbamates **12** and **13** were deprotected by acidolysis and coupled to azide-substituted glycosyl carbonate **8**. Protected derivatives **14** and **15** were de-*O*-acetylated and the azide was reduced to the amine by hydrogenolysis. Finally, the nitroxide **16**[2] activated as a succinimidyl ester was attached to yield $\mathbf{1}_1$ and $\mathbf{2}_1$, respectively.

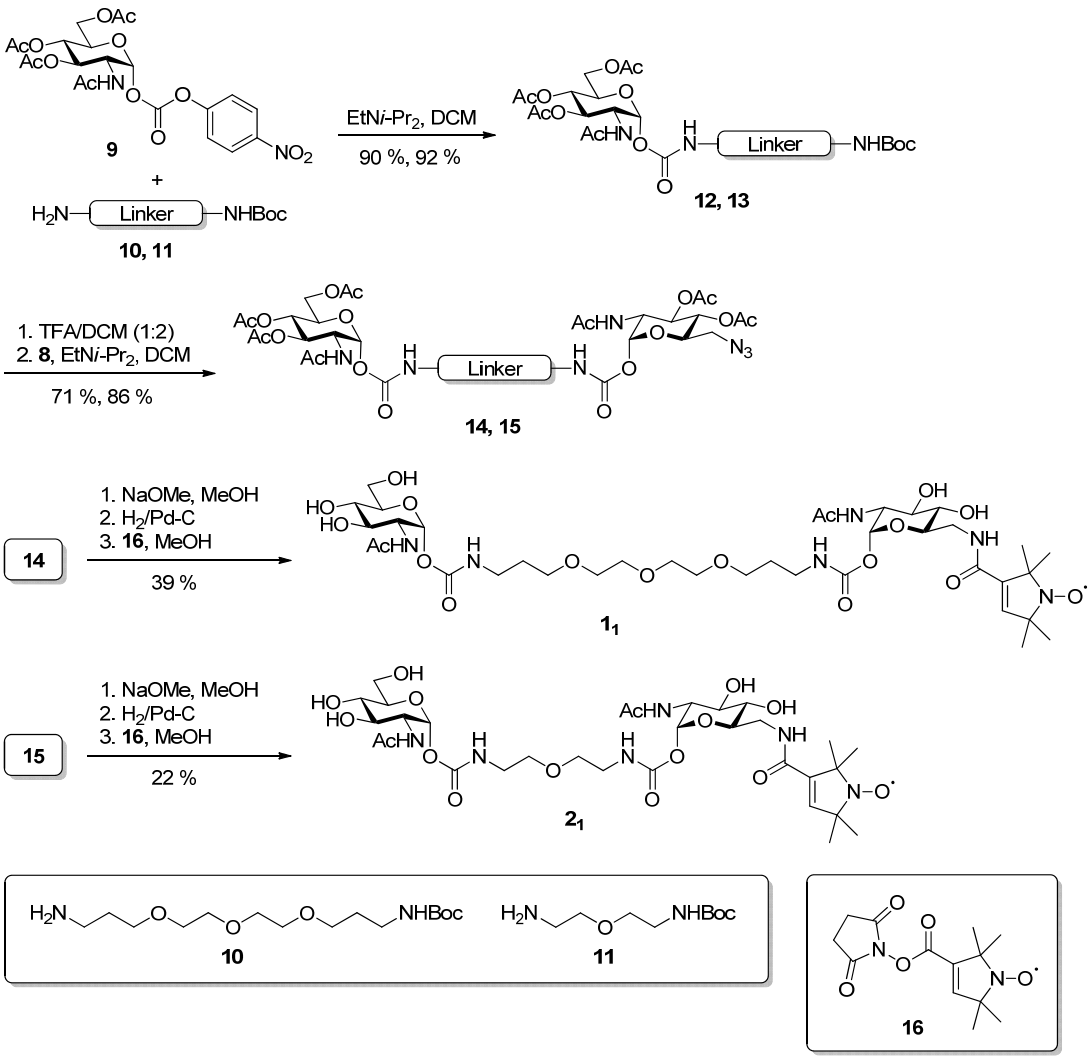

Scheme S2. Synthesis of singly spin-labeled ligands $\mathbf{1_1}$ and $\mathbf{2_1}$.

Synthesis of doubly spin-labeled ligands $\mathbf{1_2}$ and $\mathbf{2_2}$

The synthesis of doubly spin-labeled ligands $\mathbf{1_2}$ and $\mathbf{2_2}$ is shown in Scheme S3. Glycosyl carbonate **8** was coupled to diamines **17** and **18**, respectively, to yield protected derivatives **19** and **20**. These were de-*O*-acetylated and the azides were reduced to the amines by hydrogenolysis. Finally, nitroxide **16** was attached to yield $\mathbf{1_2}$ and $\mathbf{2_2}$, respectively.

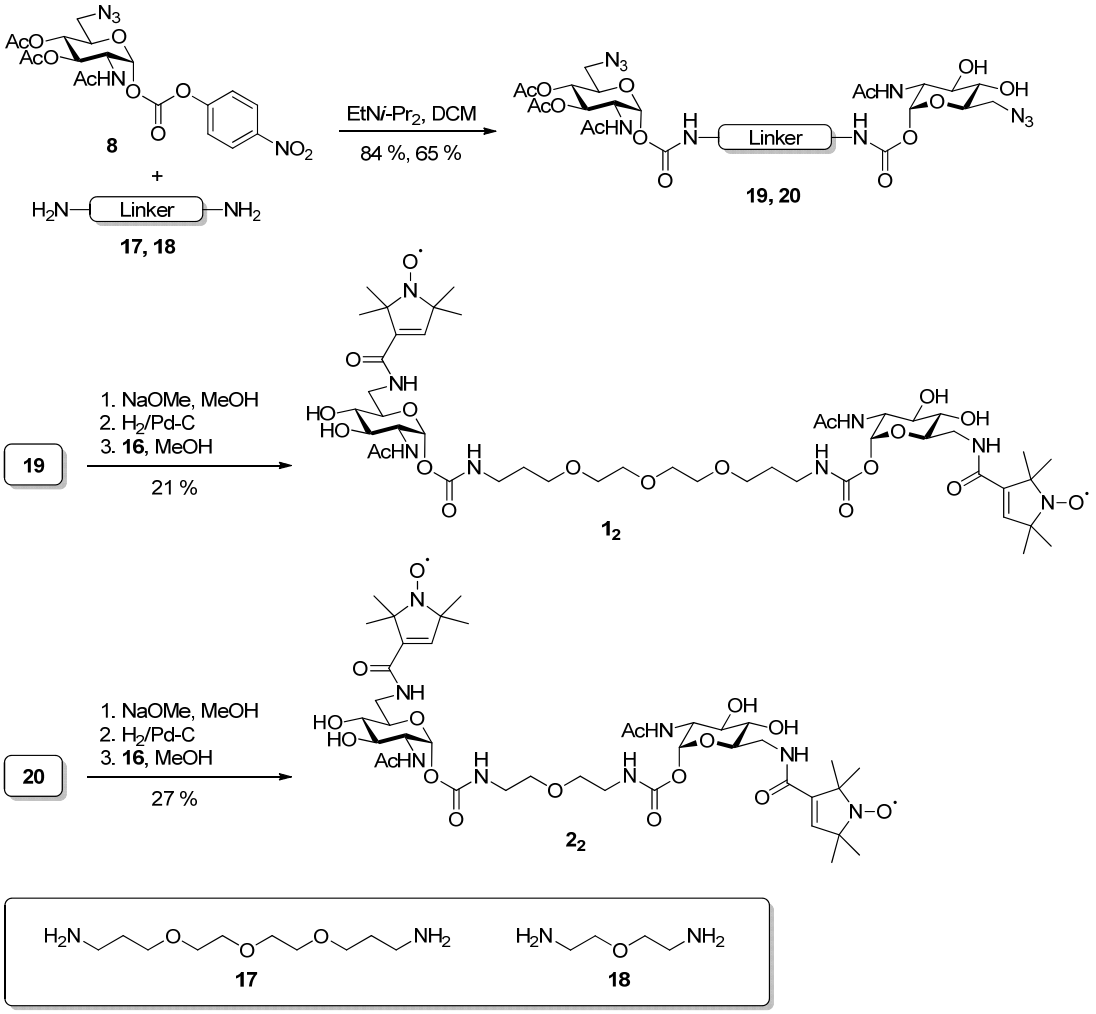

Scheme S3. Synthesis of doubly spin-labeled ligands $\mathbf{1}_2$ and $\mathbf{2}_2$.

Synthesis of singly spin-labeled ligand $\boldsymbol{3_1}$

For the synthesis of $\mathbf{3}_1$, glycosyl carbonate **8** was reacted with propylamine to yield glycosyl carbamate **21** (Scheme S4). After de-*O*-acetylation and hydrogenolysis, nitroxide **16** was coupled to give the title compound.

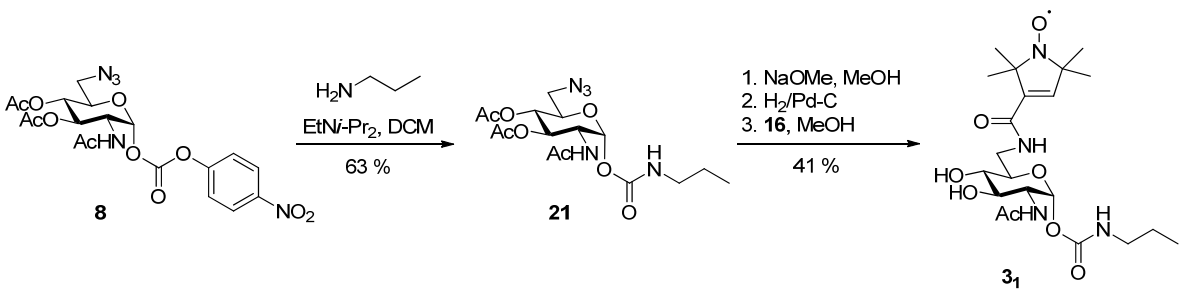

Scheme S4. Synthesis of singly spin-labeled ligand $\mathbf{3}_1$.

HPLC diagrams of purified spin-labeled ligands

Conditions: Knauer Nucleosil C18, 4 × 250 mm, flow: 1 mL min^{-1}, 10-90 % MeCN in H_2O/0.1 % TFA over 20 min

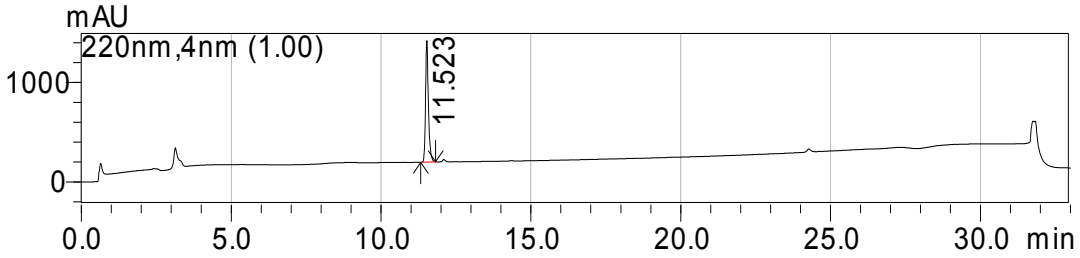

HPLC diagram of **1_1**

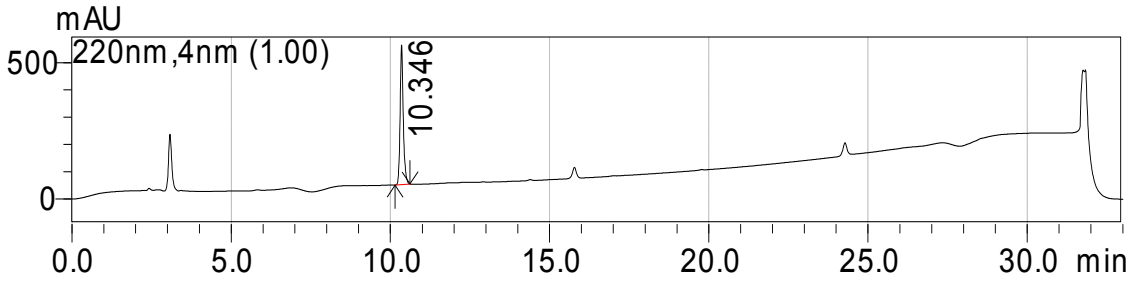

HPLC diagram of **2_1**

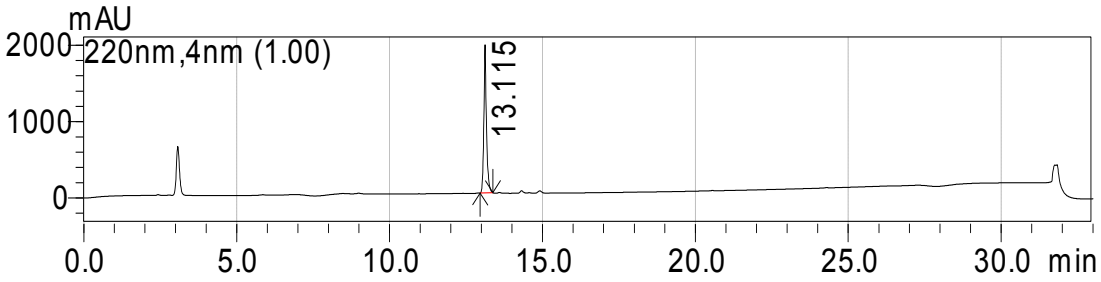

HPLC diagram of **1_2**

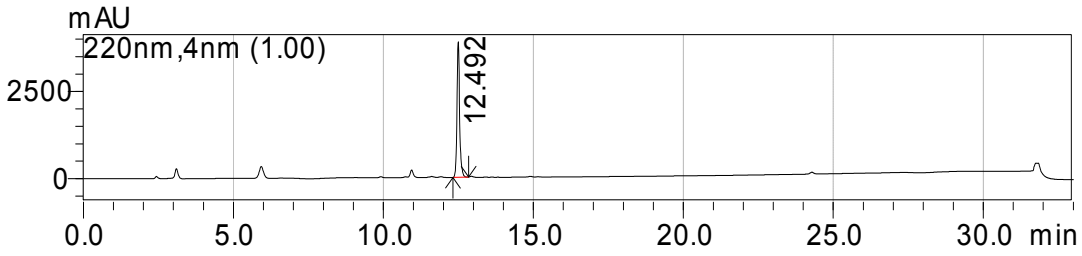

HPLC diagram of $\mathbf{2_2}$

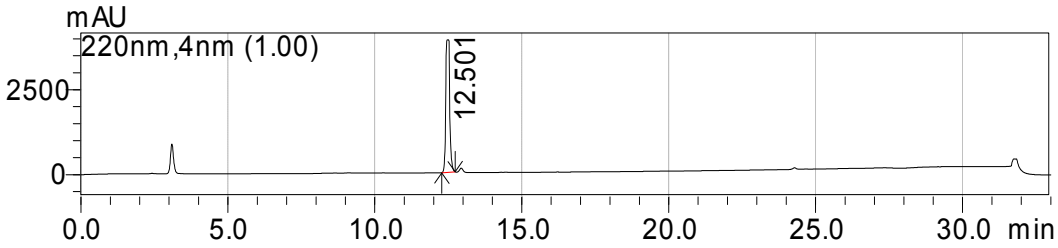

HPLC diagram of $\mathbf{3_1}$

EPR experiments

Samples were prepared by dissolution of ligands in pure water (50 μM) and addition of the corresponding amount of protein. These solutions were used for EPR measurements at room temperature. For low temperature measurements, glycerol was added to a final content of 30% (vol/vol) resulting in a ligand concentration of 33 μM and the samples were shock frozen in liquid nitrogen in order to trap the annealed conformation.

Contributions to distances below 1.5 nm in the distance distributions were detected/excluded by cw EPR measurements at T = 120 K by comparison of the doubly spin-labeled ligand with the corresponding singly labeled analog. All DEER experiments[3] were carried out at T = 40 K in X-band using a Bruker Elexsys E580 instrument equipped with a split-ring resonator. The magnetic field and the pump frequency were adjusted such that the pump π-pulse (length: 12 ns) was applied to the maximum intensity band of the nitroxide spectrum and in the centre of the resonator mode. The observer frequency was increased by 67.2 MHz with respect to the pump frequency. Pulse lengths of the observer channel were 16 and 32 ns for π/2- and π-pulses, respectively. A phase cycle (+x)-(–x) was applied to the first observer pulse. The complete pulse sequence is given by: $\pi/2_{obs}$-τ_1-π_{obs} -t-π_{pump}-(τ_1+τ_2-t)-π_{obs}-τ_2-echo. The DEER time-traces for ten different τ_1 values spaced by 8 ns starting at τ_1 = 200 ns were added in order to suppress proton modulations. Typical accumulation times per sample were 10 hours.

Data Analysis

In order to analyze the data and extract the distance distributions, the software package DeerAnalysis2009[4] has been used. Distance distributions were subjected to a data validation procedure. Experimental background functions were derived from individually measured DEER traces of corresponding singly labeled ligands if applicable.

To compare the results with the crystal structure, electronic structure modeling of $\mathbf{1_2}$ was performed using Gaussian03 (Gaussian Inc.). The conformation of **1** bound to WGA was taken from the crystal structure (Figure S4 A), the hydroxy groups in the 6-positions of the GlcNAc residues were replaced by the energy-minimized spin label. In order to estimate the width of the spin-spin distance distribution, the distance between the oxygen of the nitroxy groups was monitored versus rotating around the C_5–C_6 bond (Figure S5) without taking steric effects due to the protein into account.

Since it turned out that deconvolution of the low temperature cw EPR spectra in order to derive distance distributions did not work robust in our case, the spectral second moment $<\Delta B^2>$ was used to quantify line broadening $<\Delta\Delta B^2>$ using a home-written Matlab algorithm.[5] Corresponding values are listed in Table S1. cw EPR spectra at room temperature were analyzed using Easyspin.[6]

Table S1: Parameters from the second moment analysis for singly (i = 1) and doubly (i = 2) labeled ligands.

	$<\Delta B^2>$ (T^2), i = 1	$<\Delta B^2>$ (T^2), i = 2	$<\Delta\Delta B^2>$ (T^2)
$\mathbf{1}_i$ in absence of WGA	$2.9 \cdot 10^{-6}$	$4.7 \cdot 10^{-6}$	$1.8 \cdot 10^{-6}$
$\mathbf{1}_i$ WGA dimer / ligand 8:1	$3.4 \cdot 10^{-6}$	$3.5 \cdot 10^{-6}$	$0.1 \cdot 10^{-6}$
$\mathbf{1}_i$ WGA dimer / ligand 4:1	$3.4 \cdot 10^{-6}$	$3.7 \cdot 10^{-6}$	$0.3 \cdot 10^{-6}$
$\mathbf{2}_i$ in absence of WGA	$3.3 \cdot 10^{-6}$	$4.3 \cdot 10^{-6}$	$0.9 \cdot 10^{-6}$
$\mathbf{2}_i$ WGA dimer / ligand 8:1	$3.2 \cdot 10^{-6}$	$4.3 \cdot 10^{-6}$	$1.1 \cdot 10^{-6}$

References

[1] D. Schwefel, C. Maierhofer, J. G. Beck, S. Seeberger, K. Diederichs, H. M. Möller, W. Welte, V. Wittmann, *J. Am. Chem. Soc.* **2010**, *132*, 8704-8719.

[2] B. Hoffman, P. Schofield, A. Rich, *Proc. Natl. Acad. Sci. U. S. A.* **1969**, *62*, 1195-1202.

[3] M. Pannier, S. Veit, A. Godt, G. Jeschke, H. W. Spiess, *J. Magn. Reson.* **2000**, *142*, 331-340.

[4] a) G. Jeschke, *Macromol. Rapid Commun.* **2002**, *23*, 227-246; b) G. Jeschke, A. Koch, U. Jonas, A. Godt, *J. Magn. Reson.* **2002**, *155*, 72-82.

[5] F. Scarpelli, M. Drescher, T. Rutters-Meijneke, A. Holt, D. T. S. Rijkers, J. A. Killian, M. Huber, *J. Phys. Chem. B* **2009**, *113*, 12257-12264.

[6] S. Stoll, A. Schweiger, *J. Magn. Reson.* **2006**, *178*, 42-55.